0031-3998/11/7006-0589
PEDIATRIC RESEARCH

Vol. 70, No. 6, 2011
*Printed in U.S.A.*

# Granulocyte-Colony Stimulating Factor Alleviates Perinatal Hypoxia-Induced Decreases in Hippocampal Synaptic Efficacy and Neurogenesis in the Neonatal Rat Brain

WU-FU CHEN, JONG-HAU HSU, CHIEN-SENG LIN, YUH-JYH JONG, CHUN-HWA YANG, LIH-TUNG HUANG, AND SAN-NAN YANG

*Department of Neurosurgery [W.-F.C.], Pediatrics [L.-T.H.], Kaohsiung Chang Gung Memorial Hospital, Chang Gung University College of Medicine, Kaohsiung 807, Taiwan; Graduate Institute of Medicine [C.-H.Y.] Kaohsiung Medical University, Kaohsiung 807, Taiwan; Department of Pediatrics [J.-H.H., S.-N.Y., Y.-Y.J.], Kaohsiung Medical University Hospital, Kaohsiung 807, Taiwan; Department of Emergency and Critical Care Medicine [C.-S.L.], Cheng Hsin Rehabilitation Medical Center, Taipei 112, Taiwan*

**ABSTRACT:** Using various animal models, studies have greatly expanded our understanding of perinatal hypoxia-induced neuronal injury in the newborn at the cellular/molecular levels. However, the synapse-basis pathogenesis and therapeutic strategy for such detrimental alterations in the neonatal brain remain to be addressed. We investigated whether the damaged synaptic efficacy and neurogenesis within hippocampal CA1 region (an essential integration area for mammalian learning and memory) of the neonatal rat brain after perinatal hypoxia were restored by granulocyte-colony stimulating factor (G-CSF) therapy. Ten-day-old (P10) rat pups were subjected to experimentally perinatal hypoxia. G-CSF (10, 30, or 50 $\mu$g/kg, single injection/d, P11–16) was s.c. administered to neonatal rats which were analyzed on P17. Perinatal hypoxia reduced the expression in *p*Raf-*p*ERK1/2-*p*CREB$^{Ser\text{-}133}$ signaling, the synaptic complex of postsynaptic density protein-95 (PSD-95) with *N*-methyl-D-aspartate receptor (NMDAR) subunits (NR1, NR2A, and NR2B), synaptic efficacy, and neurogenesis. A representatively effective dosage of G-CSF (30 $\mu$g/kg) alleviated the perinatal hypoxia-induced detrimental changes and improved the performance in long-term cognitive function. In summary, our results suggest a novel concept that synaptic efficacy defects exist in the neonatal brain previously exposed to perinatal hypoxia and that G-CSF could be a clinical potential for the synapse-basis recovery in the perinatal hypoxia suffers. **(*Pediatr Res* 70: 589–595, 2011)**

Cerebral hypoxia induced by asphyxia episodes during the neonatal period leads to long-term neurologic disabilities varying from mild behavioral dysfunctions to severe seizure, mental retardation, and/or CP among the newborn (1). Studies indicated that transient cerebral hypoxia triggered a series of pathophysiological changes leading, ultimately, to the neurodegeneration in oxygen sensitive so-affected brain regions, including the hippocampus (an important integration area for mammalian cognitive learning and memory) (2–4). Although underlying mechanisms for the neonatal brain following perinatal hypoxia are extensively studied in the past, it remains unclear about synapse-basis pathogenesis and effective drug therapy.

Phosphorylation of cAMP-responsive element-binding protein at serine 133 [phosphorylated cAMP-responsive element-binding protein at serine 133 (*p*CREB$^{Ser\text{-}133}$), a neurotrophic nuclear transcription factor] is involved in the formation of the synaptic complex of postsynaptic density 95 (PSD-95) protein with the *N*-methyl-D-aspartate receptor (NMDAR) subunit and serves important roles in the neurological regulation of ion-channel function, neuronal differentiation and maturation, synaptogenesis, synaptic plasticity, neuronal survival, and the processes of learning and memory (5–12). Previously, we reported that, using an animal model, experimentally perinatal hypoxia decreased *p*CREB$^{Ser\text{-}133}$ and PSD-95 expression within the hippocampus (9,13). Thus, it highlights the possibility that such decreased expression could be a tentative therapeutic target for an alleviation of long-term neurological dysfunctions.

Granulocyte-colony stimulating factor (G-CSF), a 19.6-kDa glycoprotein, has been approved for clinical use to treat neutropenia in humans (14). G-CSF facilitated bone marrow cell mobilization to the brain and drove neurogenesis and reduced infarct volume with improved functional outcome in adult animals immediately after experimentally stroke insult (15–24). Furthermore, G-CSF exerted neurotrophic effects through binding to the specific G-CSF receptor (G-CSFR) on neuronal cells (22). However, most studies primarily focused on acute application of G-CSF therapy in the adult stroke brain or cell culture model, giving little clue of whether G-CSF *in vivo* provides beneficial effects with synaptic efficacy recovery in the neonatal brain after perinatal hypoxia. Here, we reported, using a neonatal animal model, G-CSF exerted neurotrophic activity involving *p*Raf-*p*ERK1/2-*p*CREB$^{Ser\text{-}133}$ pathway, synaptic efficacy, and neurogenesis recovery.

Received April 20, 2011; accepted July 2, 2011.

Correspondence: San-Nan Yang, M.D., Ph.D., Department of Pediatrics, Kaohsiung Medical University Hospital, Graduate Institute of Medicine, Kaohsiung Medical University, No. 100, Zihyou 1st Road, Sanmin District, Kaohsiung City 807, Taiwan; e-mail: y520729@gmail.com

Supported by grants from the National Science Council, Taiwan (NSC 98-2320-B-037-022-MY3) and Kaohsiung Medical University Hospital (KMUH-97-7R06, KMUH99-9R-38 and KMUH-6R-23), Taiwan.

The authors report no conflicts of interest.

**Abbreviations: BrdU,** bromodeoxyuridine; **G-CSF,** granulocyte-colony stimulating factor; **LTP,** long-term potentiation; **NeuN,** neuronal nuclei; **NMDAR,** *N*-methyl-D-aspartate receptor; **pCREB$^{Ser\text{-}133}$,** phosphorylated cAMP-responsive element-binding protein at serine 133; **pERK1/2,** extracellular signal-regulated kinase ½; **pRaf,** phosphorylated mitogen-activated protein-kinase-kinase-kinase; **PSD-95,** postsynaptic density 95

## MATERIALS AND METHODS

***Experimental animal protocols.*** All experimental procedures were approved by the Animal Care and Use Committee at Kaohsiung Medical University (Kaohsiung, Taiwan) and National Science Council (Taipei, Taiwan). Sprague-Dawley (SD) rats were housed in the animal-care facility provided with a 12-h light/dark cycle. On postnatal day 9 (P9), the animals were divided into four experimental groups as follows: vehicle-control, G-CSF alone, perinatal hypoxia, and G-CSF plus perinatal hypoxia rats, respectively. The procedures for inducing perinatal hypoxia were as described previously (9,13,25). It is generally accepted that rat pups of P10 to P12 roughly correspond to a term human infant (26). Briefly, rats (P10) were removed from the litter and placed in an airtight chamber (30 × 30 × 30 cm) on a heating pad to maintain temperature at 34°C. After this, the $O_2$ concentration was reduced to 5 to 7% and maintained at this level by constant, regulated infusion of $N_2$ gas into the chamber. Only rats exhibiting at least one tonic-clonic seizure and lower blood oxygen saturation (<60%) during hypoxia were used for this study. One day after induction of perinatal hypoxia, rat pups were s.c. injected with recombinant human G-CSF (Kyowa Hakko Kirin Co., Tokyo, Japan) or vehicle-saline (P11–16), as experimental design needed.

***Hippocampal slice preparation.*** On P17, hippocampal slices (400 μm) were collected and were immediately transferred to artificial cerebrospinal fluid (ACSF) in an incubating chamber featuring a humidified 95% $O_2$/5% $CO_2$ gas at 34.0 ± 0.5°C for an equilibrium period of at least 1 h (9,13,25). To obtain hippocampal CA1 region tissue, a hippocampal slice was incubated with ice-cold oxygenated ACSF and was then cut into a tissue block (0.1 × 0.5 cm) within 15 s of tissue slicing. Subsequently, hippocampal CA1 tissues were immediately frozen at −80°C until analysis was undertaken, and all such tissue was only ever thawed once.

***Evaluation of protein expression.*** Hippocampal CA1 tissues (P17) were used for coimmunoprecipitation analyses in the synaptic complex of PSD-95 with NMDAR subunit (NR1, NR2A, and NR2B), and nuclear protein extracts with cytoplasmic supernatant were collected as described previously (9,13,25). The synaptic membranous components of PSD-95 and the NMDAR subunits (the P2 membrane fractions) of the homogenates were centrifuged at 800 g for a period of 10 min at 4°C. The supernatants were combined and centrifuged at 11,000 g at 4°C for 20 min to obtain the synaptic P2 pellet. This synaptic pellet was then resuspended in 0.32 M sucrose containing phosphatise/protease inhibitor kit (Roche Molecular Biochemicals, Germany) (4,9,13,25). The protein concentrations were measured by the use of Bio-Rad DC protein-assay kits (Cat. No. 500-0112, Bio-Rad Laboratories, Hercules, CA). Subsequently, coimmunoprecipitation was performed with the Catch and Release Immunoprecipitation System (Upstate Biotechnology, Lake Placid, NY). A quantity of protein (500 μg) was incubated with a specific antibody and antibody capture-affinity ligand for 15 min at room temperature and then transferred onto spin columns. Samples were then loaded onto 10% SDS-polyacrylamide gels and resolved by standard electrophoresis (Novex, Carlsbad, CA). The gels were then transferred onto PVDF filters that had been incubated with a specific primary antibody: phosphorylated mitogen-activated protein-kinase-kinase-kinase (*p*Raf; 1:1000), extracellular signal-regulated kinase 1/2 (*p*ERK1/2; 1: 1000), *p*CREB$^{Ser\text{-}133}$ (1:1,000), PSD-95 (1:2,000), and the NR1, NR2A, NR2B (1:1,000) subunits of NMDARs (Upstate Biotechnology). Subsequently, the filters were stripped and reprobed with anti-total CREB (1:1,000) or anti-β-tubulin (1:2,000) both of which served as the internal standard (Upstate). For quantification of immunoblot signals, the band intensity was measured using a Kodak Digital Science 1D program (Rochester, NY).

***Evaluation of neurogenesis.*** To identify the expression of cell type-specific markers in bromodeoxyuridine (BrdU)-positive cells and neurogenesis, double-immunofluorescence analysis of laser-scanning confocal microscopy was performed as previously described (9,18,20). On P17, the brains were cut coronally at 30 μm and brain sections were washed for 20 min in PBS containing 0.2% Triton X-100, pH 7.3, at room temperatures with gentle rocking and then incubated for 1 h at room temperature in blocking solution with gentle rocking. Cell proliferation induced G-CSF was detected by BrdU injection (P14–16, 50 mg/kg/q12 h, s.c.). The expressions of neuronal nuclei-(NeuN) and BrdU-positive double immunofluoresence were tested following the instructions of the Roche BrdU labeling and detection kit. Each coronal section was first treated with primary BrdU antibody conjugated with FITC (1:250) staining, followed by treatment with neuron-specific antibody (NeuN; 1:500, Chemicon, Temecula, CA). The tissue sections were analyzed with an Olympus laser-scanning confocal microscope, and green (FITC) and red (Cy3) fluorochromes on the slides were excited by laser beam at 488 and 543 nm, respectively.

***Evaluation of synaptic efficacy.*** Bipolar stimulating electrodes were positioned in Schaffer/commissural pathways at a distance within 100 μm from the cell body layer of CA1 pyramidal cells of hippocampus from the animals (P17) to stimulate mainly proximal apical dendritic synapses (25). The cell membrane potential was held at −65 mV throughout the experiments. Monophasic constant voltage pulses (0.2 ms) were delivered at a frequency of 0.1 Hz to Schaffer/commissural fibers. In long-term potentiation (LTP) experiments, high frequency stimulation (HFS) was applied to Schaffer fibers (three 100 Hz bursts, each 1 s in duration and spaced 1 min s apart) in which membrane potential was held at −40 mV for the duration of the tetanus.

***Evaluation of long-term cognitive function.*** An open-field water maze (2 m in diameter; opaque water; 28 ± 1°C; automated swim-path monitoring) was applied in this study to characterize long-term learning and memory (9,25). Visible platform-trained: rats were trained to a randomly located platform (30 cm diameter) position marked with a striped flag protruding above, such training being conducted between P37 and P39 inclusively [four trials per day for 3 d; curtains drawn around the pool to occlude extra-maze cues; maximum trial duration was 90 s; intertrial interval (ITI), 10 min]. For hidden-platform training, a hidden platform with the extra-maze cues visible was used between P40 and P44 inclusively (four trials per day for a period of 5 days; platform per pool area was 1/44; a period of 30 s was allowed for test animals on the platform at the end of each trial; ITI, 10 min). On P45, the measure of time spent in the annular zone within the training quadrant was observed as a final record.

In this study, all data were presented as mean ± SEM. Statistical differences were determined by use of a one-way ANOVA followed by a Bonferroni's *t* test for *post hoc* multiple comparisons. A statistical significance level $p < 0.05$ was applied to all tests.

## RESULTS

***Synaptic PSD-95 expression.*** This study first investigated whether G-CSF therapy exerts beneficial effect in the decreased expression of synaptic PSD-95 within hippocampal CA1 region in the neonatal brain after perinatal hypoxia. As indicated in Figure 1*A*, G-CSF therapy (10, 30, or 50 μg/kg), with a representatively effective dosage at 30 μg/kg, significantly attenuated the perinatal hypoxia-induced decrease in PSD-95 expression on P17. We promptly studied whether a phosphorylated cascade of signaling pathway (*p*Raf-*p*ERK1/2-*p*CREB$^{Ser\text{-}133}$) was associated to this synaptic PSD-95 alteration (27,28). Figure 1 (*B–D*) revealed that an application of G-CSF (30 μg/kg) concomitantly reversed the perinatal hypoxia-induced decrease in phosphorylated activity of *p*Raf-*p*ERK1/2-*p*CREB$^{Ser\text{-}133}$ pathway ($p < 0.05$).

***Synaptic complex of PSD-95 with NMDAR subunit expression.*** Because synaptic PSD-95 dynamically links to NMDAR subunit (5–9,13), this study further examined that the synaptic stoichiometry of protein interaction between synaptic PSD-95 and NMDAR subunit (NR1, NR2A, and NR2B) could be modulated by such G-CSF therapy. When PSD-95 was the immunoprecipitating antibody, the amounts of NR1, NR2A, and NR2B that coprecipitated with PSD-95 were all reduced in the perinatal hypoxia group ($p < 0.05$), especially with the largest decrease in the synaptic complex of PSD-95 and NR2A (Fig. 2*B*). In contrast, G-CSF therapy significantly alleviated the perinatal hypoxia-induced decrease in the expression of synaptic complex of PSD-95 with NMDAR subunit. In addition, the decreased expression in total protein levels for NR1, NR2A, and NR2B was seen in the perinatal hypoxia group and was reversed by G-CSF therapy.

***Synaptic efficacy.*** This study further determined whether the functional expression of synaptic efficacy within hippocampal CA1 region of rats (P17) was altered by perinatal hypoxia and/or G-CSF therapy. Hippocampal LTP (8,25), a form of NMDAR-mediated synaptic activity with a persistent enhancement in synaptic efficacy underlying mammalian

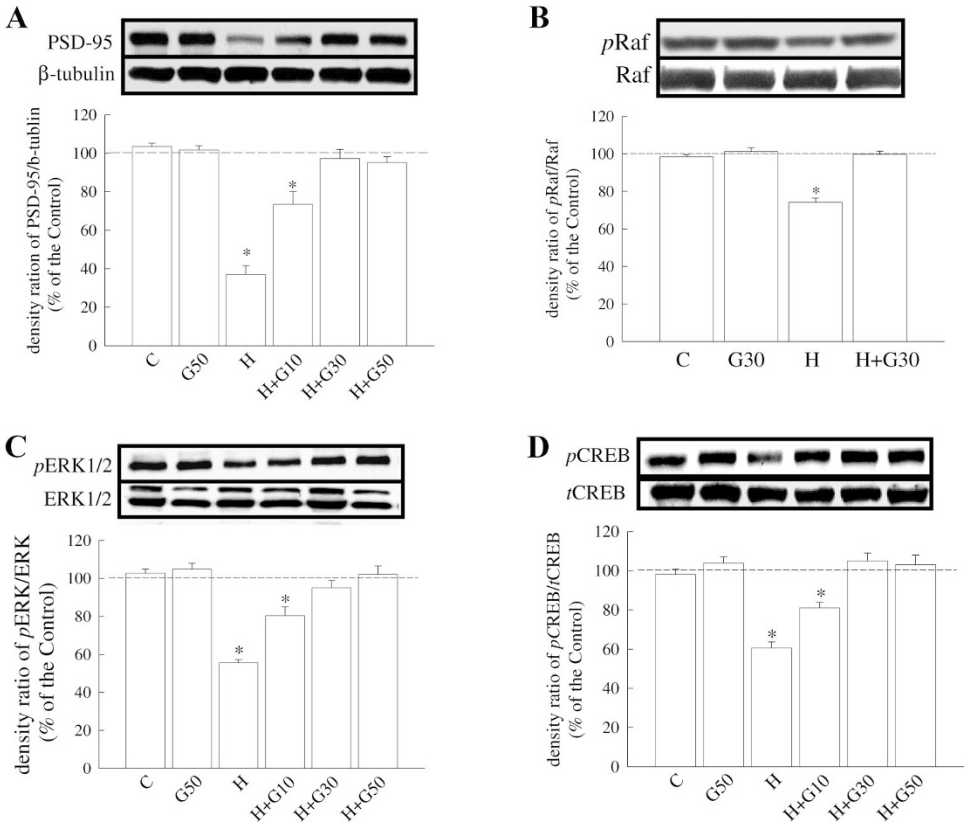


**Figure 1.** The decreased expression in PSD-95 and phosphorylated signaling (*p*Raf-*p*ERK1/2-*p*CREB$^{Ser\text{-}133}$) after perinatal hypoxia was attenuated by G-CSF therapy. Summary of normalized *p*Raf-*p*ERK1/2-*p*CREB$^{Ser\text{-}133}$-PSD-95 pathway in the neonatal brain, as determined on P17. Perinatal hypoxia-induced decreases in the expression of (*A*) PSD-95, (*B*) *p*Raf, (*C*) *p*ERK1/2, and (*D*) *p*CREB$^{Ser\text{-}133}$ were reversed by G-CSF therapy with a representatively effective dosage at 30 $\mu$g/kg. The Raf, ERK1/2, CREB, and $\beta$-tubulin served as internal standard controls for each experimental group, respectively. The labels for vehicle-control, G-CSF (10, 30, or 50 $\mu$g/kg) alone, perinatal hypoxia, and perinatal hypoxia plus G-CSF (30 $\mu$g/kg) groups are C, G, H, and H + G, respectively ($n = 8$ animals for each experimental group). *$p < 0.05$ when compared with the vehicle-control group.

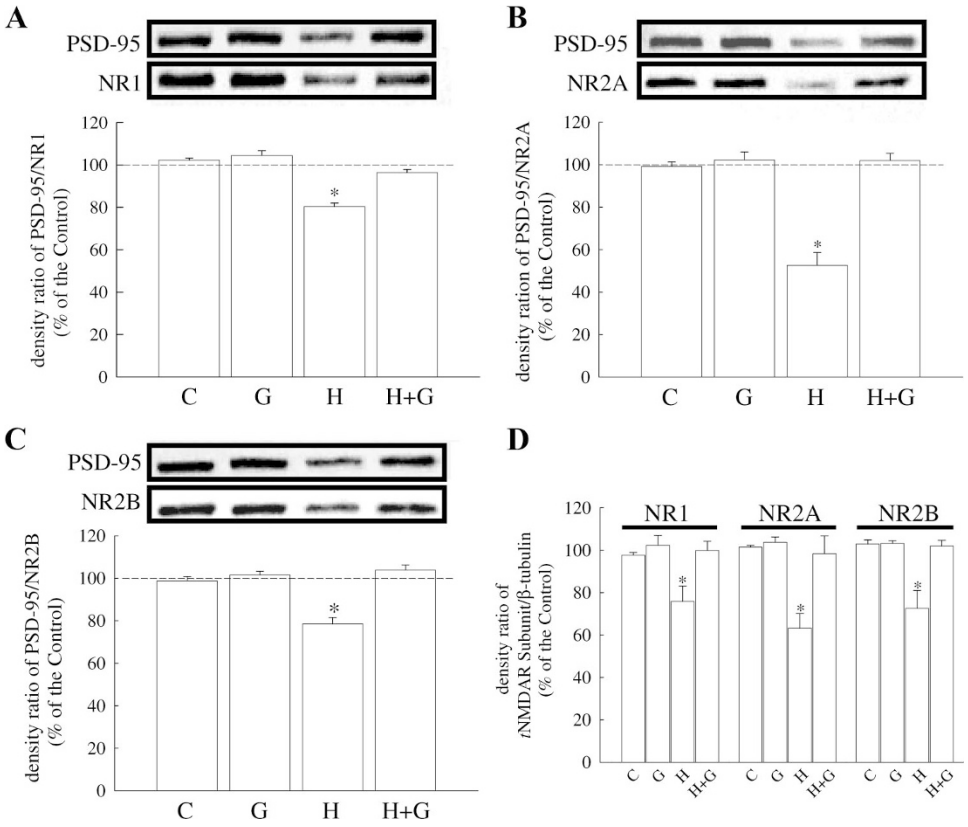


**Figure 2.** Perinatal hypoxia-induced decreased expression in synaptic complex of PSD-95 with NMDAR subunit was alleviated by G-CSF therapy. Summary of the normalized ratios for (*A*) PSD-95/NR1, (*B*) PSD-95/NR2A, and (*C*) PSD-95/NR2B with representative coimmunoprecipitations, respectively. The synaptic complex of PSD-95 with NMDAR subunit was obtained from a same rat on P17, for a total of 10 animals per experimental group. (*D*) Summary of total protein levels of NR1, NR2A, and NR2B subunits of NMDARs in rats, as assessed at P17. The labels for vehicle-control, G-CSF (30 $\mu$g/kg) alone, perinatal hypoxia, and perinatal hypoxia plus G-CSF (30 $\mu$g/kg) groups are C, G, H, and H + G, respectively ($n = 6$ animals for each experimental group). *$p < 0.05$ when compared with the vehicle-control group.

learning and memory, was used in this study. As demonstrated in Figure 3, a decreased magnitude of LTP expression was seen in the perinatal hypoxia group. In contrast, G-CSF therapy significantly reversed the perinatal hypoxia-induced decrease in the magnitude of LTP expression, compared with the vehicle-control group ($p < 0.05$).

***Neurogenesis.*** We next assessed whether the G-CSF therapy enhanced the expression of neurogenesis within hippocampal

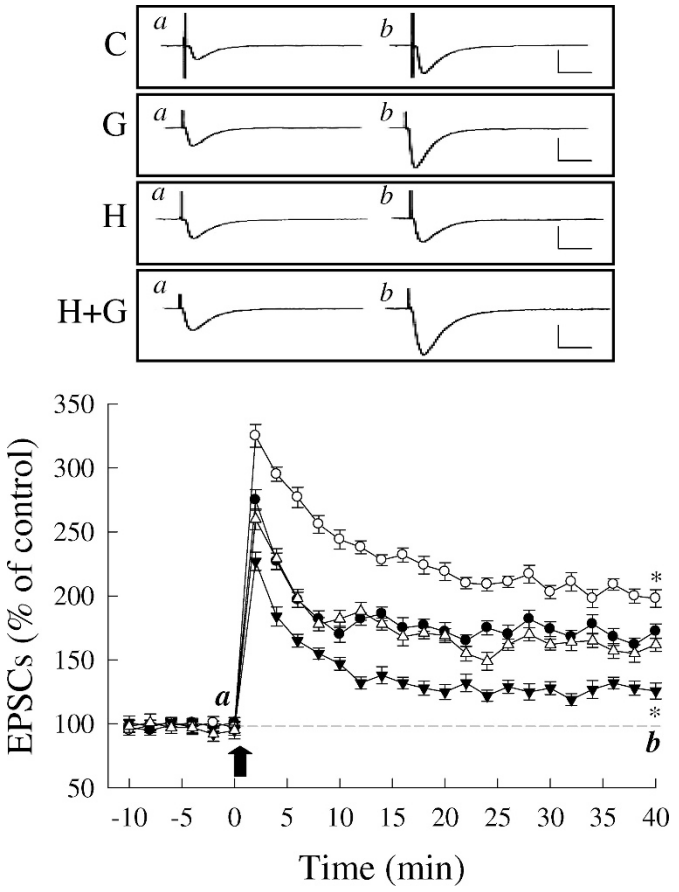


**Figure 3.** Impaired synaptic efficacy-induced perinatal hypoxia was improved by G-CSF therapy. Expression of hippocampal LTP induced in slices using high-frequency stimulation (HFS) in rats (P17). A conventional HFS protocol (HFS, one 100 Hz bursts, 1 s in duration), starting at time point 0 min (the *arrow* sign) was applied to the slices of vehicle-control (*C*, ●), 30 μg/kg G-CSF alone (*G*, ○), perinatal hypoxia (*H*, ▼), and perinatal hypoxia plus 30 μg/kg G-CSF groups (H + G, △) groups ($n = 10$ slices from five animals for each experimental group). At the holding potential of −60 mV, representative traces of excitatory postsynaptic currents (EPSCs) recorded in the same neuron before (inset *a*) and 40 min after HFS (inset *b*) from each experimental group. Calibration: 200 pA (vertical line)/50 ms (horizontal line). *$p < 0.05$ represents statistical difference compared with the vehicle-control group.

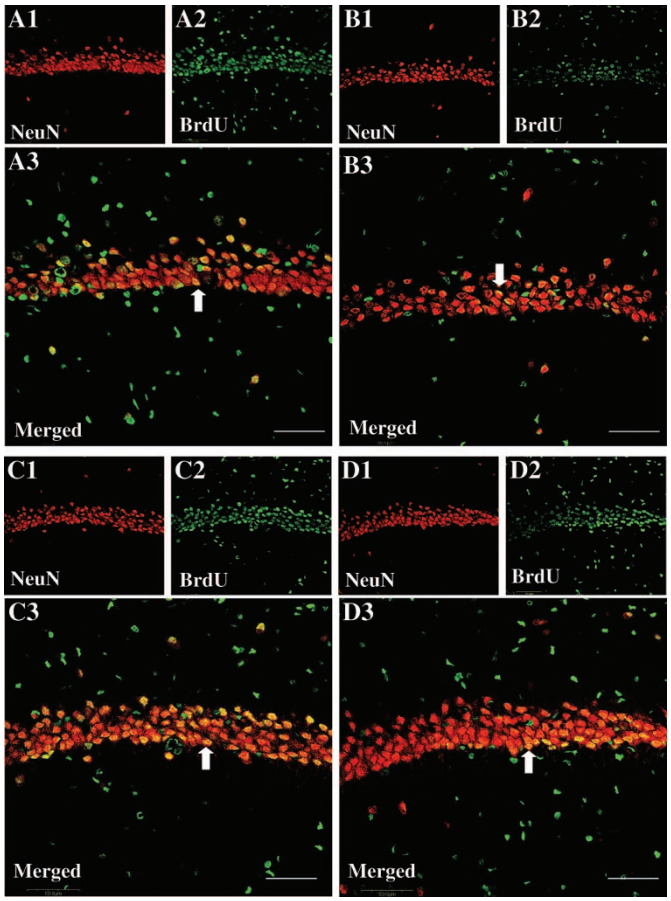


**Figure 4.** Effects of G-CSF therapy in the decreased expression of neurogenesis induced by perinatal hypoxia. Double-immunofluorescent staining under laser-scanning confocal microscopy was used to identify colocalization of NeuN- (*red* for neuron identification) and BrdU- (*green* for cell nucleus detection) positive cells, as assessed on P17. The NeuN-positive cells were displayed as follows: (A1) vehicle-control, (B1) perinatal hypoxia, (C1) G-CSF alone (30 μg/kg), and (D1) perinatal hypoxia plus G-CSF (30 μg/kg), respectively. The BrdU-positive cells were demonstrated as follows: (A2) vehicle-control, (B2) perinatal hypoxia, (C2) G-CSF alone (30 μg/kg), and (D2) perinatal hypoxia plus G-CSF (30 μg/kg), respectively. The merged pictures of the NeuN- and BrdU cells were exhibited as follows: (A3) vehicle-control, (B3) perinatal hypoxia, (C3) G-CSF (30 μg/kg), and (D3) perinatal hypoxia plus G-CSF (30 μg/kg), respectively. The *arrow* insets show the representatively new-generated neurons. Bar = 50 μm.

CA1 region in the neonatal brain after perinatal hypoxia. A decreased trend in coexpressing of BrdU-positive with NeuN-positive cells was observed in the perinatal hypoxia group ($p < 0.05$; Fig. 4*B*), when compared with vehicle-control rats. In contrast, the G-CSF plus perinatal hypoxia group revealed an increase number in BrdU-positive cells colocalizing NeuN-positive cells (Fig. 4*D*). As quantitative analysis in Figure 5, the average cell number exhibiting double staining with NeuN- and BrdU-positive cells within the counted areas showed that G-CSF therapy significantly reversed the perinatal hypoxia-induced decrease in neurogenesis, confirming the double staining of immunoflourescence findings in Figure 4.

***Long-term cognitive function.*** To assess whether G-CSF therapy exerted beneficial effects for an impaired performance in long-term cognitive function among test animals, the water maze task was applied at later ages (P37–45). In the NMDAR-independent cue task, the four groups learned to approach a randomly located platform marked by a visible cue with featuring an equivalent and progressive reduction in path length over successive trials ($p > 0.1$) (Fig. 6*A*). We further tested spatial learning using the hidden-platform version of the NMDAR-dependent spatial task water maze. The swim paths of animals from the neonatal asphyxia group indicated significantly longer overall path lengths, compared with the other groups ($p < 0.05$, Fig. 6*B*). There appeared to be no statistical intergroup difference in swimming speed or locomotor activity on any test day. Subsequent to 20 training trials (P45), performance at a transfer test (with the platform removed) was used as an index of retention memory (Fig. 6*C–D*). The three groups (vehicle-control, G-CSF alone, G-CSF plus perinatal hypoxia) showed a spatial bias toward the training target quadrant (dashed circles, Fig. 6*C*), spending significantly more time search there, unlike the perinatal hypoxia group. In addition, there was no statistical difference in major biochemical analyzed at P37 among the four experiments ($p > 0.1$).

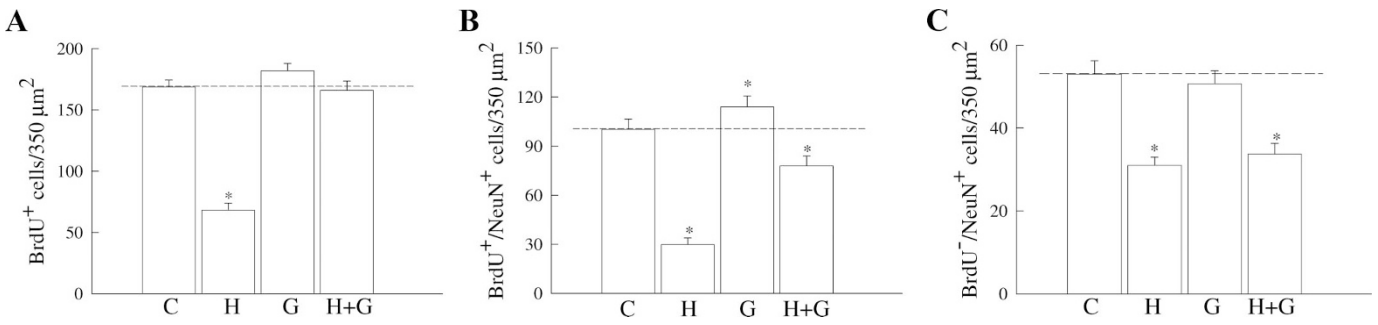


**Figure 5.** Quantified analysis for the effects of G-CSF therapy in the decreased expression of neurogenesis induced by perinatal hypoxia. (*A*) Summary of BrdU-positive cells in rats, as assessed on P17. (*B*) Summary of colocalization of NeuN- and BrdU-immunoreactive cells, as assessed on P17. (*C*) Summary of NeuN-positive and BrdU-negative cells in rats, as assessed on P17. The labels for vehicle-control, G-CSF (30 $\mu$g/kg) alone, perinatal hypoxia, and perinatal hypoxia plus G-CSF (30 $\mu$g/kg) groups are C, G, H, and H + G, respectively ($n$ = 60 sections from six animals for each experimental group). *$p < 0.05$ when compared with the vehicle-control group.

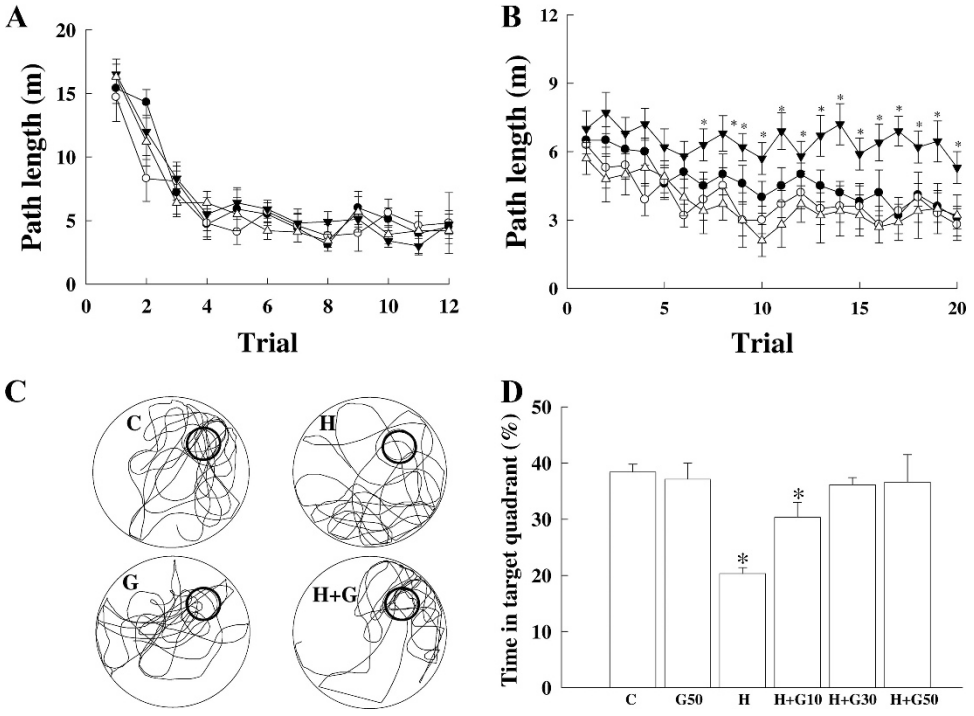


**Figure 6.** Impaired performance in long-term spatial learning and memory after perinatal hypoxia was improved by G-CSF treatment. (*A*) Path length across 3 d of training to a visible cue (four trials per d, P37–39 inclusively). By trial 12, the path lengths of the four groups in the 2 m diameter pool were equivalent and close to the minimum possible path length. (*B*) Path length across 5 d of location learning to a hidden platform (P40–44 inclusively). $n$ = 15 animals for each experimental group: vehicle-control (●), 30 $\mu$g/kg G-CSF alone (○), perinatal hypoxia (▼), and perinatal hypoxia plus 30 $\mu$g/kg G-CSF (△). *$p < 0.05$ compared with the vehicle-control group. (*C*) At P45, representative swimming path for the final behavioral recordings in which the letters for four experimental groups indicated as follows: vehicle-control (C), 30 $\mu$g/kg G-CSF alone (G), perinatal hypoxia (H), and perinatal hypoxia plus 30 $\mu$g/kg G-CSF (H + G). The three groups of rats (C, G, and H + G) learnt to take relatively direct paths, whereas the perinatal hypoxia group rats (H) persisted in taking circuitous routes. *Shaded circles* indicate hidden platforms within the target training quadrants. (*D*) Averaged proportional time spent in the target platform on P45. Note that the perinatal hypoxia group failed to search the platform in the target location even after extensive training, whereas the perinatal hypoxia plus G-CSF group searches in the correct location in a dose-dependent fashion. The labels for vehicle-control, G-CSF (50 $\mu$g/kg) alone, perinatal hypoxia, perinatal hypoxia plus 10 $\mu$g/kg G-CSF, 30 $\mu$g/kg G-CSF, and 50 $\mu$g G-CSF groups are C, G50, H, H + G10, H + G30, and H + G50, respectively. *$p < 0.05$ when compared with the vehicle-control group.

## DISCUSSION

In this study, we delineated a tentative therapy in which systemic injections of G-CSF exert beneficial effects for the neonatal rat brain after experimentally perinatal hypoxia. This therapy scheme significantly alleviated the decreased expression of *p*Raf-*p*ERK1/2-*p*CREB$^{Ser\text{-}133}$ pathway, synaptic complex of PSD-95 with NMDAR subunits (NR1, NR2A, and NR2B), synaptic efficacy, and neurogenesis in hippocampal CA1 region of the neonatal brain previously exposed to perinatal hypoxia.

Possible mechanisms underlying therapeutic benefits of G-CSF have been reported through multidimensional effects (22). The therapeutic actions of G-CSF were to be primarily mediated through the G-CSFR within the neurons of the mammalian brain (16,20). Administration of G-CSF displayed neurotrophic, anti-inflammatory, antiapoptotic, neurogenesis, and angiogenesis effects, all of which may contribute to the neuroprotective properties of G-CSF in the mammalian adult brain (15–24). However, the information currently available seems limited to suggest that these beneficial effects primarily

**Table 1.** *Long-term physiological parameter after G-CSF therapy*

| Each group (n = 10) | RBC ($10^6/\mu L$) | WBC ($10^6/\mu L$) | BUN (mg/dL) | Cr (mg/dL) | AST (U/L) | ALT (U/L) | Glucose (mg/dL) | Na (mEq/L) | K (mEq/L) | Ca (mEq/L) |
|---|---|---|---|---|---|---|---|---|---|---|
| C | 6.3 ± 0.2 | 8.2 ± 0.7 | 18.2 ± 0.9 | 0.3 ± 0.05 | 301 ± 23 | 75 ± 4 | 136 ± 12 | 138 ± 1.1 | 7.2 ± 0.3 | 10.7 ± 0.2 |
| H | 6.6 ± 0.2 | 8.6 ± 1.1 | 17.6 ± 0.9 | 0.3 ± 0.02 | 269 ± 19 | 74 ± 7 | 130 ± 9 | 138 ± 0.9 | 7.5 ± 0.1 | 10.4 ± 0.2 |
| G | 6.5 ± 0.1 | 8.8 ± 1.2 | 17.4 ± 0.8 | 0.4 ± 0.04 | 306 ± 30 | 75 ± 7 | 146 ± 10 | 139 ± 1.1 | 8.1 ± 0.3 | 10.7 ± 0.1 |
| H + G | 6.6 ± 0.2 | 9.1 ± 0.7 | 16.2 ± 0.7 | 0.4 ± 0.03 | 295 ± 29 | 79 ± 4 | 142 ± 9 | 136 ± 1.9 | 7.9 ± 0.3 | 10.8 ± 0.2 |

Values are mean ± SEM.

C, vehicle-control; H, perinatal hypoxia; G, G-CSF; H + G, perinatal hypoxia plus G-CSF; RBC, red blood cell; WBC, white blood cell; BUN, blood urea nitrogen; Cr, creatinine; AST, aspartate aminotransferase; ALT, alanine aminotransferase; Eq, equivalent.

existed in cell culture and/or adult animal stroke model. Here, this study includes the first examination of the effects of G-CSF in which G-CSF therapy significantly enhanced synapse-basis recovery and contributed a beneficial role for the perinatal hypoxia-induced neurological deficit.

Phosphorylated CREB$^{Ser\text{-}133}$ contributes to functional/morphological synaptogenesis, synaptic plasticity, and neuronal survival with neurogenesis in the CNS (29–31). Here, we provided experimental evidence that a decrease in *p*CREB$^{Ser\text{-}133}$ and PSD-95 expression resulting from perinatal hypoxia was reversed by the G-CSF therapy (Fig. 1). Previous studies suggest that CREB is a member of a family of DNA-binding transcription factors and is involved in the transcriptional regulation of certain immediated-early genes (32). Although acute administration of G-CSF increased the number of newly generated neurons in the adult brain immediately after ischemic-hypoxic animal model (15–24), most experimental therapies for ischemic-hypoxic models described above primarily focus on reducing the size of ischemic-hypoxic damage and on rescuing dying cells nearly after occurrence in adult animals. In such adult animal models, available treatments were often limited by a very narrow therapeutic time window, and limited information has been shown to enhance the synaptic function recovery when G-CSF therapy was initiated for the neonatal brain. Here, in this study, the G-CSF therapy promoted the expression of the neurotrophic signaling pathway (*p*Raf-*p*ERK1/2-*p*CREB$^{Ser\text{-}133}$) leading to a restoration of synaptic efficacy with neurogenesis after perinatal hypoxia, and hence provided beneficial effect for long-term cognitive deficits without introducing unwanted side effects (Fig. 6, Table 1). However, it is worth noting that this study does not necessarily exclude a potential role of bone marrow stem cells, which could stimulate the production of critical neurotrophic substances (15–24). In addition, the G-CSF alone group (30 $\mu$g/kg) significantly increased a greater extent for the efficacy of LTP (Fig. 3) but not for the expression of synaptic protein (Figs. 1 and 2). Thus, further experiments are needed to confirm a closer link between the western blot and the electrophysiology findings in individual neurons seen in this study.

In conclusion, this study supports that the G-CSF therapy was able to promote a combined beneficial mechanism involving neurogenesis with synaptic efficacy recovery, and, at least in part, improve the long-term functional outcome in rats suffering from perinatal hypoxia (33). A useful neuroprotective strategy should be well tolerated, not interfere with essential physiology in the developing brain after hypoxia episodes, and approaches pathophysiological mechanisms in parallel to improve long-term cognitive outcomes. Although specific extrapolation of the results of rodent experiments to the neonatal human condition appears difficult, our results could suggest a new potential therapeutic strategy for neurological deficits in the patients suffering from neonatal hypoxia.

## REFERENCES


1. du Plessis AJ, Volpe JJ 2002 Perinatal brain injury in the preterm and term newborn. Curr Opin Neurol 15:151–157
2. Oler JA, Markus EJ 1998 Age-related deficits on the radial maze and in fear conditioning: hippocampal processing and consolidation. Hippocampus 8:402–415
3. Mizuno M, Yamada K, Olariu A, Nawa H, Nabeshima T 2000 Involvement of brain-derived neurotrophic factor in spatial memory formation and maintenance in a radial arm maze test in rats. J Neurosci 20:7116–7121
4. Lin CS, Tao PL, Jong YJ, Chen WF, Yang CH, Huang LT, Chao CF, Yang SN 2009 Prenatal morphine alters the synaptic complex of PSD-95 with NMDA receptor subunit in hippocampal CA1 subregion of rat offspring leading to long-term cognitive deficits. Neuroscience 158:1326–1337
5. Yamada Y, Chochi Y, Takamiya K, Sobue K, Inui M 1999 Modulation of the channel activity of the $\epsilon 2/\zeta 1$-subtype N-methyl-D-asparate receptor by PSD-95. J Biol Chem 274:6647–6652
6. Kennedy MB 2000 Signal-processing machines at the postsynaptic density. Science 290:750–754
7. Takagi N, Logan R, Teves L 2000 Altered interaction between PSD-95 and the NMDA receptor following transient global ischemia. J Neurochem 74:169–178
8. Köhr G 2006 NMDA receptor function: subunit composition versus spatial distribution. Cell Tissue Res 326:439–446
9. Chen WF, Chang H, Wong CS, Huang LT, Yang CH, Yang SN 2007 Impaired expression of postsynaptic density proteins in the hippocampal CA1 region of rats following perinatal hypoxia. Exp Neurol 204:400–410
10. Bender RA, Luterborn JC, Gall CM, Cariage W, Baram TZ 2001 Enhanced phosphorylation in immature dentate gyrus cells precedes neutrophin expression and indicates a specific role of CREB in granule cells differentiation. Eur J Neurosci 13:679–686
11. Kandel ER 2001 The molecular biology of memory storage: a dialogue between genes and synapses. Science 294:1030–1038
12. Mayr B, Montminy M 2001 Transcriptional regulation by the phosphorylation-dependent factor CREB. Nat Rev Mol Cell Biol 2:599–609
13. Chen WF, Chang H, Huang LT, Yang CH, Lai MC, Wan TH, Yang SN 2006 Alterations in long-term seizure susceptibility and the complex of PSD-95 with NMDA receptor from animals previously exposed to perinatal hypoxia. Epilepsia 47:288–296
14. Frampton JE, Lee CR, Faulds D 1994 Filgrastim. A review of its pharmacological properties and therapeutic efficacy in neutropenia. Drugs 48:731–760
15. Heard SO, Fink MP 1999 Counterregulatory control of the acute inflammatory response: granulocyte colony-stimulating factor has anti-inflammatory properties. Crit Care Med 27:1019–1021
16. Schäbitz WR, Kollmar R, Schwaninger M, Juettler E, Bardutzky J, Schölzke MN, Sommer C, Schwab S 2003 Neuroprotective effect of granulocyte colony-stimulating factor after focal cerebral ischemia. Stroke 34:745–751
17. Sheibani N, Grabowski EF, Schoenfeld DA, Whalen MJ 2004 Effect of granulocyte colony-stimulating factor on functional and histopathologic outcome after traumatic brain injury in mice. Crit Care Med 32:2274–2278
18. Shyu WC, Lin SZ, Yang HI, Tzeng YS, Pang CY, Yen PS, Li H 2004 Functional recovery of stroke rats induced by granulocyte colony-stimulating factor-stimulated stem cells. Circulation 110:1847–1854
19. Gibson CL, Jones NC, Prior MJ, Bath PM, Murphy SP 2005 G-CSF suppresses edema formation and reduces interleukin-1beta expression after cerebral ischemia in mice. J Neuropathol Exp Neurol 64:763–769
20. Schneider A, Kruger C, Steigleder T, Weber D, Pitzer C, Laage R, Aronowski J, Maurer MH, Gassler N, Mier W, Hasselblatt M, Kollmar R, Schwab S, Sommer C, Bach A, Kuhn HG, Schabitz WR 2005 The hematopoietic factor G-CSF is a

neuronal ligand that counteracts programmed cell death and drives neurogenesis. J Clin Invest 115:2083–2098
21. Ohki Y, Heissig P, Sato Y, Akiyama H, Zhu Z, Hicklin DJ, Shimada K, Ogawa H, Daida H, Hattori K, Ohsaka A 2005 Granulocyte colony-stimulating factor promotes neovascularization by releasing vascular endothelial growth factor from neutrophils. FASEB J 19:2005–2007
22. Solaroglu I, Jadhav V, Zhang JH 2007 Neuroprotective effect of granulocyte-colony stimulating factor. Front Biosci 12:712–724
23. Yata K, Matchett GA, Tsubokawa T, Tang J, Kanamaru K, Zhang JH 2007 Granulocyte-colony stimulating factor inhibits apoptotic neuron loss after neonatal hypoxia-ischemia in rats. Brain Res 1145:227–238
24. Minnerup J, Heidrich J, Wellmann J, Rogalweski A, Schneider A, Schäbitz WR 2008 Meta-analysis of the efficacy of granulocyte-colony stimulating factor in animal models of focal cerebral ischemia. Stroke 39:1855–1861
25. Yang SN, Huang LT, Wang CL, Chen WF, Yang CH, Lin SZ, Lai MC, Chen SJ, Tao PL 2003 Prenatal administration of morphine decreases CREBSerine-133 phosphorylation and synaptic plasticity range mediated by glutamatergic transmission in the hippocampal CA1 area of cognitive-deficient rat offspring. Hippocampus 13:915–921
26. Romijn HJ, Hofman MA, Gramsbergen A 1991 At what age is the developing cerebral cortex of the rat comparable to that of the full-term newborn human baby? Early Hum Dev 26:61–67
27. Impey S, Obrietan K, Wong ST, Poser S, Yano S, Wayman G, Deloulme JC, Chan G, Storm DR 1998 Cross talk between ERK and PKA required for Ca2+ stimulation of CREB-dependent transcription and ERK nuclear translocation. Neuron 21:869–883
28. Impey S, Obrietan K, Storm DR 1999 Making new connections: role of ERK/MAP kinase signaling in neuronal plasticity. Neuron 23:11–14
29. Bito H, Takemoto-Kimura S 2003 Ca(2+)/CREB/CBP-dependent gene regulation: a shared mechanism critical in long-term synaptic plasticity and neuronal survival. Cell Calcium 34:425–430
30. Tojima T, Ito E 2004 Signal transduction cascades underlying de novo protein synthesis required for neuronal morphogenesis in differentiating neurons. Prog Neurobiol 72:183–193
31. Garoflos E, Stamatakis A, Mantelas A, Philippidis H, Stylianopoulou F 2005 Cellular mechanisms underlying an effect of "early handling" on pCREB and BDNF in the neonatal rat hippocampus. Brain Res 1052:187–195
32. Hughes PE, Alexi T, Walton M, Williams CE, Dragunow M, Clark RG, Gluckman PD 1999 Activity and injury-dependent expression of inducible transcription factors, growth factors and apoptosis-related genes within the central nervous system. Prog Neurobiol 57:421–450
33. Lie DC, Song H, Colamarino SA, Ming GL, Gage FH 2004 Neurogenesis in the adult brain: new strategies for central nervous system diseases. Annu Rev Pharmacol Toxicol 44:399–421